RSC Advances

ROYAL SOCIETY OF CHEMISTRY

www.rsc.org/advances

A fast charging/discharging all-solid-state lithium ion battery based on PEO-MIL-53(Al)-LiTFSI thin film electrolyte

Kai Zhu, Yexiang Liu and Jin Liu*

School of Metallurgy and Environment, Central South University, Changsha City, 410083, China

*Corresponding author: Jin Liu
Email: jinliu@csu.edu.cn

Metal-organic framework aluminum 1,4-benzenedicar-boxylate (MIL-53(Al)) is used as a filler for polyethylene oxide (PEO) based thin film electrolyte. With the participation of MIL-53(Al), the ionic conductivity of this electrolyte is increased from 9.66×10^{-4} S cm^{-1} to 3.39×10^{-3} S cm^{-1} at 120 ^{o}C and the electrochemical window is raised from 4.99 V to 5.10 V. Besides, the all-solid-state $LiFePO_4$/Li battery based on the electrolyte was fabricated. At 5 C and 120 ^{o}C, the battery delivers the discharge capacity of 136 mAh g^{-1} in the initial cycle, 129 mAh g^{-1} in the 300th cycle, and 83.5 mAh g^{-1} in the 1400th cycle. At 10 C and 120 ^{o}C, its discharge capacity is 116.2 mAh g^{-1} in the initial cycle and 103.5 mAh g^{-1} in the 110th cycle. The results indicate that this metal-organic framework (MIL-53(Al)) is a novel structural modifier for solid polymer electrolyte in fast charging/discharging lithium ion batteries.

1 Introduction

All-solid-state polymer lithium ion batteries (LIBs) have higher safety than conventional LIBs since liquid flammable electrolyte is replaced by solid electrolyte.[1-5] However, the cycle performance of batteries assembled by such solid polymer electrolyte does not have a strong appeal when batteries are charged/discharged at high current densities. Generally, the fast charging/discharging capability of a battery is determined by subjecting the battery to high charging/discharging rates that about 40% of the state of charge/discharge must be obtained within 15 min (about 1.6 C rate).[6] This requires that conductible ions in the electrolyte can transport quickly between two electrodes.[7] Thus, various studies were focused on the improvement of ionic conductivity of solid polymer electrolyte,[8,9] especially on the modification of polyethylene oxide (PEO) based electrolyte.[10-18] For example, the ionic conductivity was increased to 2.0×10^{-4} S cm^{-1} at 80 ^{o}C by adding silane-treated Al_2O_3.[16] The $LiFePO_4$/Li battery assembled by this electrolyte showed the discharge capacity of 140 mAh g^{-1} in the 100th cycle at 0.2 C and 90 ^{o}C. In 2013, we reported the PEO based electrolyte with metal-organic-framework-5 (MOF-5) as filler for all-solid-state $LiFePO_4$/Li battery.[17] The ionic conductivity increased to 7.9×10^{-4} S cm^{-1} from 3.9×10^{-4} S cm^{-1} at 75 ^{o}C. The battery attained the initial discharge capacity of 151 mAh g^{-1} and 45% capacity retention in the 100th cycle at 1 C and 80 ^{o}C. However, it did not charge/discharge at higher rates. One of the reasons would be from strong absorption of MOF-5 for water and small molecules, resulting in instability of the electrolyte. Recently, another MOF aluminium (III)-1,3,5-benzenetricarboxylate (Al-BTC) was reported as a filler for added to PEO based electrolyte.[18] The ionic conductivity of ~7×10^{-4} S cm^{-1} at 70 ^{o}C was measured. The $LiFePO_4$/Li battery with the electrolyte delivered the specific capacity of about 100 mAh g^{-1} at 2 C and 70 ^{o}C. At 5 C, the battery had low specific capacity of 40 mAh g^{-1}.

MOFs are inorganic-organic hybrid materials that were primarily applied in the fields of drug delivery, optoelectronics, sensing and catalysis.[19-22] Aluminum 1,4-benzenedicar-boxylate (MIL-53(Al)) is one of the MOFs which is built of corner-sharing $AlO_4(OH)_2$ octahedra.[23] It has remarkable water and oxygen stability compared to MOF-5.[24] In this study, the PEO based electrolyte was prepared by using MIL-53(Al) as filler and lithium bis(trifluoro-methanesulfonyl)imide (LiTFSI) as lithium salt. Its ionic conductivity is 3.39×10^{-3} S cm^{-1} at 120 ^{o}C that is higher than 9.66×10^{-4} S cm^{-1} of that without MIL-53(Al). The $LiFePO_4$/Li battery based on this electrolyte has an average discharge capacity of 103.5 mAh g^{-1} for 110 cycles at a high rate of 10 C and 120 ^{o}C, demonstrating potentials of the modified PEO electrolyte based lithium ion battery in faster charging/discharging applications.

2 Experimental

2.1 Preparation of MIL-53(Al) nano-particles

Aluminum 1,4-benzenedicar-boxylate (MIL-53(Al)) nano particles were synthesized under hydrothermal conditions by treating 1,4-benzenedicarboxylate acid (H_2BDC, 99%), N,N-dimethylformamide (DMF, +99.9%), deionized water with aluminum nitrate nonahydrate ($Al(NO_3)_3\ 9H_2O$, 98%).[23] The materials were stirred for 2h, and then transferred to a Teflon-lined steel autoclave (50 mL). The autoclave was heated in an oil bath at 160 ^{o}C for 50 h. The free H_2BDC and water in the sample were removed by washing with absolute alcohol and filtering for 3 times. The sample was heated in a vacuum at 120 ^{o}C for 12 h to obtain white powder product.

2.2 Preparation of thin film electrolytes

The polyethylene oxide (PEO, M_W 4×10^6, 99.9%) was thoroughly dried at 50 ^{o}C for 12 h, and the lithium bis(trifluoro-methanesulfonyl)imide ($LiN(SO_2CF_3)_2$, LiTFSI, +99.5%) was dried at 100 ^{o}C in

a vacuum for 24 h before use. Firstly, LiTFSI was added to the acetonitrile (CH_3CN, AR grade) and stirred for 2 h. Then, MIL-53(Al) nano-particles were added to the solution and stirred for 10 min. After that, PEO was dispersed into the solution and stirred for 36 h. The result was a homogenized colloidal solution. Finally, the solution was cast and dried into a thin film at 80 ^oC for 24 h in an argon-filled gloved box, and a PEO-MIL-53(Al)-LiTFSI thin film electrolyte formed. Using this electrolyte, all-solid-state $LiFePO_4$/Li batteries were fabricated for all evaluations.

2.3 Characterization and instruments

The surface morphology of MIL-53(Al) nano-particle and thin film electrolyte were observed with scanning electron microscope (SEM, sirion 200). The X-ray diffraction (XRD, RINT-2000, Rigaku) patterns were collected from a Rigaku/TTR-III powder diffractometer equipped with Cu-Kα radiation (λ =1.5418Å) at 25 ^oC. The diffraction pattern range was recorded from 5^o to 60^o with a step of 10^o min^{-1}. Thermogravimetric analysis (TG) was carried out on Perkin-Elmer Pyris-1. The thin film electrolytes were loaded in hermetically sealed aluminum pans, and measurements were carried out at a heating rate of 10 ^oC min^{-1} from 48 ^oC to 500 ^oC. The mechanical strength of the thin film electrolytes was measured by Shimadzu TA Q800-1706 instrument with a tensile speed of 1 N min^{-1}.

The electrochemical properties of the electrolytes were measured by using a PARSTAT 2273 system (PerkinElmer Instrument, USA). Electrochemical window was determined using blocking stainless steel electrode/electrolyte/Li batteries at a scan rate of 10 mV s^{-1} from 2.5 V to 6.5 V. The ionic conductivities were determined by the AC impedance spectroscopy which was carried out in the 500 KHz to 10 Hz frequency range. The equation for calculating the conductivity is

$$\sigma = \frac{d}{R_p S}$$

where the d is the thickness of the electrolyte, R_p is the resistance of the electrolyte and is the intercept in X-axis of the straight line in the low frequency range, and the S is the area of the blocking stainless steel electrodes.

The lithium ion transference number of the electrolyte was tested in a symmetric cell (Li/electrolytes/Li) by using PARSTAT 2273. The symmetric Li/electrolyte/Li battery was polarized at a small voltage of 10 mV. AC impedance plots of the cell before and after polarization were obtained.

The cycling performance of all-solid-state $LiFePO_4$/electrolyte/Li batteries was investigated by using the $LiFePO_4$/electrolyte/Li batteries. The charging/discharging cycles of the batteries were performed on a Land instrument (Wuhan Land Electronic Co., Ltd. China), and the tests used the cut-off voltages of 4.0 V (charge) and 2.5 V (discharge). All the batteries were assembled in an argon-filled UNILAB glove box.

3 Results and discussion

3.1 Characteristics of MIL-53(Al) nano particles and PEO-MIL-53(Al)-LiTFSI thin film electrolyte.

Fig. 1a shows the XRD pattern of MIL-53(Al) in which the characteristic peaks of the sample are identical with the pattern simulated by the lattice parameters of MIL-53(Al).[23] The surface morphologies of MIL-53(Al) and PEO-MIL-53(Al)-LiTFSI thin film electrolyte were investigated by SEM. Cylindrical nano particles in the MIL-53(Al) sample and an uniform surface for the electrolyte are respectively observed in Fig.1b and Fig. 1c, suggesting that the cylindrical particles would not damage the architecture of the thin film.

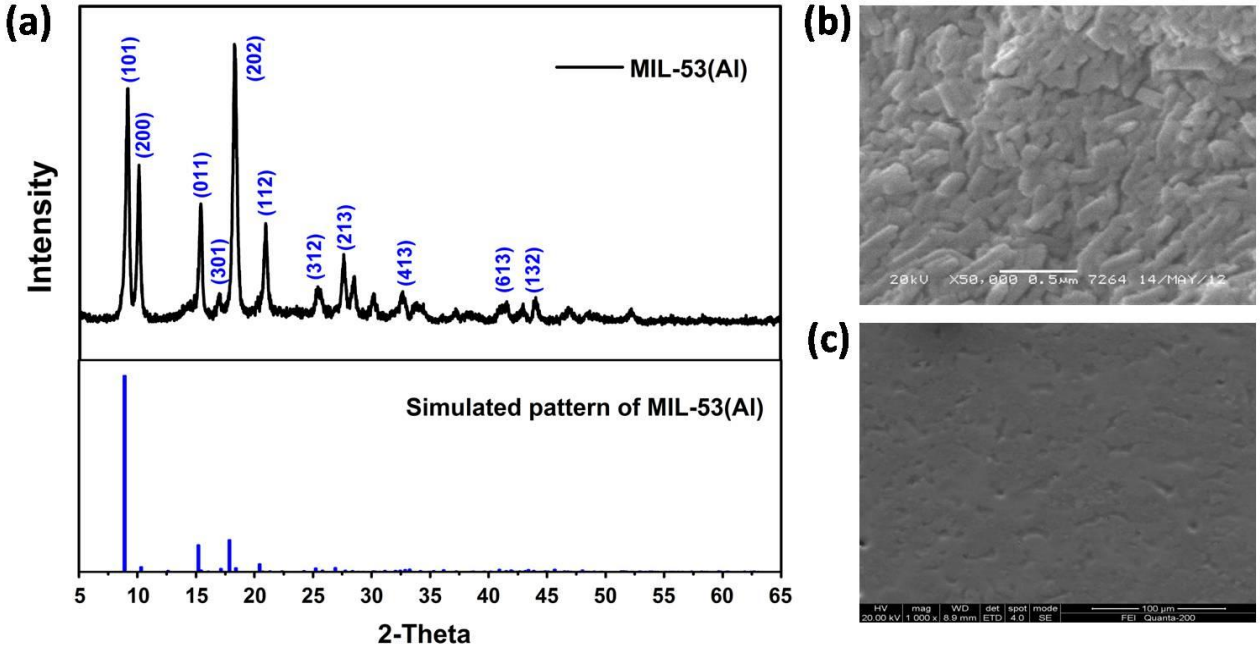

Fig. 1 (a) XRD pattern of MIL-53(Al) and the simulated pattern based on the crystallographic data of MIL-53(Al),[23] (b) SEM images of MIL-53(Al) and (c) the PEO-MIL-53(Al)-LiTFSI thin film electrolyte.

3.2 Lithium ionic conductivities of thin film electrolytes

The ionic conductivities of the thin film electrolytes with different EO (ethylene oxide in PEO):Li molar ratios and different MIL-53(Al) concentrations at 30 ^{o}C, 60 ^{o}C and 80 ^{o}C were measured, and the results are listed in Table 1. At a fixed MIL-53(Al) concentration of 10 wt%, the electrolyte with the EO:Li ratio of 15:1 has the highest ionic conductivities at the three temperatures compared to the other ratios of 10:1, 20:1 and 25:1. At the constant EO:Li ratio of 15:1 and various MIL-53(Al) concentrations of 0, 10 and 20 wt%, there are the highest ionic conductivities at 10 wt% MIL-53(Al) and at the three temperatures. Hence, the EO:Li ratio of 15:1 and the MIL-53(Al) concentration of 10 wt% were selected as optimized parameters for the preparation of the electrolyte.

Table 1 Ionic conductivities at 30 ^{o}C, 60 ^{o}C, and 80 ^{o}C for the PEO-Xwt%MIL-53(Al)-LiTFSI thin film electrolytes with different EO:Li ratios.

EO:Li	X	Ionic conductivities (S cm^{-1})

		30 °C	60 °C	80 °C
10:1	10	1.29×10^{-5}	4.30×10^{-4}	9.03×10^{-4}
15:1	10	1.62×10^{-5}	4.48×10^{-4}	9.71×10^{-4}
20:1	10	3.36×10^{-6}	8.41×10^{-5}	1.68×10^{-4}
25:1	10	1.14×10^{-6}	6.60×10^{-5}	1.65×10^{-4}
15:1	0	6.35×10^{-7}	4.70×10^{-5}	9.24×10^{-5}
15:1	20	1.13×10^{-6}	2.63×10^{-5}	2.41×10^{-4}

Previous studies found that the ionic conduction behavior is different in the crystalline phase and amorphous phase of the PEO based electrolyte, and the ionic conductivity is higher in the amorphous phase than in the crystalline phase.[25] In order to determine the phase transition temperature and find the applicable operating temperature range of the PEO-MIL-53(Al)-LiTFSI electrolyte, the ionic conductivities at 40 °C, 45 °C, 50 °C, 55 °C, 60 °C, 65 °C, 70 °C, 80 °C, 100 °C, 120 °C and 150 °C were measured (see Fig. 2). The ionic conductivity of the electrolyte is 3.39×10^{-3} S cm^{-1} at 120 °C that is 3.5 times compared to the PEO-LiTFSI electrolyte without MIL-53(Al) (9.66×10^{-4} S cm^{-1}) at the same EO:Li ratio of 15:1. Meanwhile, at low temperatures, the log σ shows a linear relation with 1/T, while at high temperatures, a nonlinear relation is presented. By fitting the data with the Arrhenius equation ($\sigma = A\exp\frac{E_a}{RT}$)[26] at low temperatures and the Vogel-Tamman-Fulcher (VTF) equation ($\sigma = AT^{-0.5}\exp[-\frac{B}{k(T-T_0)}]$)[27] at high temperatures, the phase transition temperatures of 50.3 °C for the PEO-MIL-53(Al)-LiTFSI electrolyte and 56.9 °C for the PEO-LiTFSI electrolyte are obtained, where σ is the ionic conductivity, A is the pre-exponential factor, E_a is the pseudo activation energy for ionic transport, R is the gas constant, k is the Boltzman constant, B is the pseudo activation energy, T is the test absolute temperature, and T_0 is the equilibrium glass transition

temperature. There is a decrease of 6.6 ^{o}C in the phase transition temperature. This is ascribed to the addition of MIL-53(Al), leading to the higher ionic conductivities of the PEO-MIL-53(Al)-LiTFSI electrolyte. In addition, above the phase transition temperatures, both the electrolytes are amorphous and the ionic conductivities are higher. These results indicate that the ionic conduction behavior is indeed related to the phase structure.

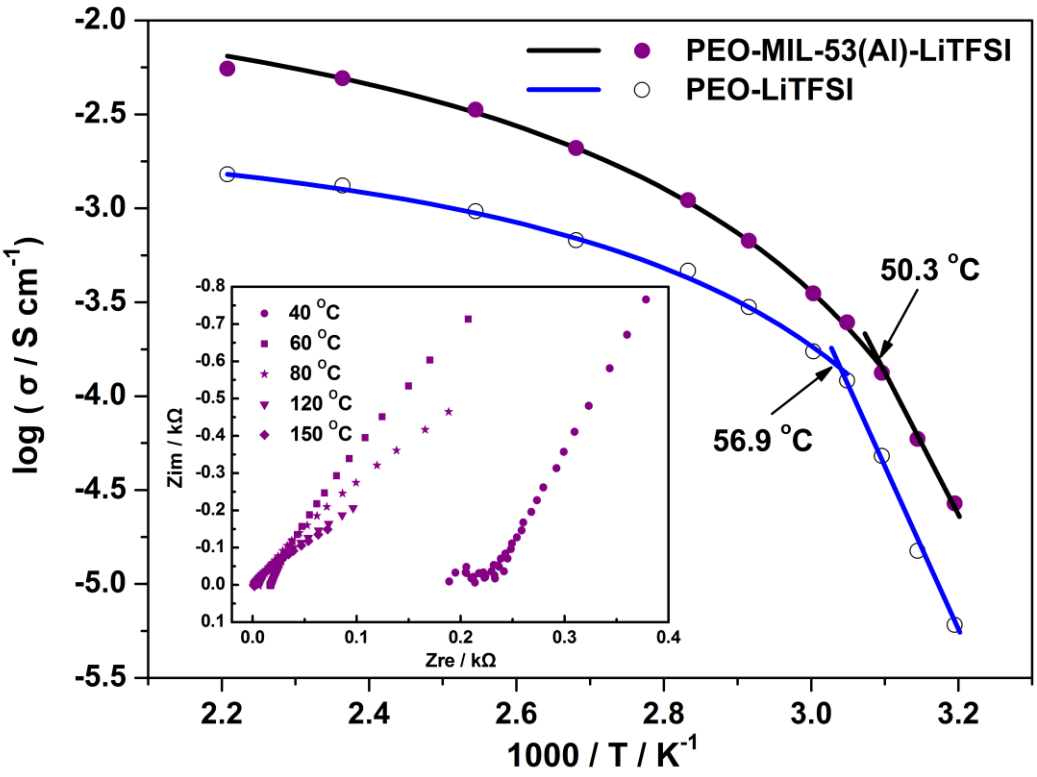

Fig. 2 Temperature dependent conductivities for the PEO-10wt%MIL-53(Al)-LiTFSI electrolyte and the PEO-LiTFSI electrolyte at the same EO:Li ratio of 15:1. The circles are the experimental data and the lines are the fitted results.[28,29] Inset: the AC impedance spectra of the PEO-MIL-53(Al)-LiTFSI electrolyte at selected temperatures of 40 ^{o}C, 60 ^{o}C, 80 ^{o}C, 120 ^{o}C and 150 ^{o}C.

The lithium ion transference number, t^{+}, is another desirable parameter of electrolytes.[30,31] The measurement of t^{+} was carried out by using the AC impedance spectroscopy and the chronoamperometry (CA). Fig. 3 shows the relation between time and current crossing a symmetric

Li/PEO-MIL-53(Al)-LiTFSI/Li battery polarized by a small voltage of 10 mV at 80 ^{o}C. The inset is the AC impedance spectra of the same battery before and after the polarization. Then, the t^{+} can be calculated by the following equation[32]:

$$t^{+} = \frac{I_{ss}}{I_0}\frac{(\Delta V - I_0 R_0)}{(\Delta V - I_{ss} R_{ss})}$$

where I_0 and I_{ss} are the initial current and the steady-state current, respectively, ΔV is the voltage, R_0 and R_{ss} are the initial and steady-state interfacial resistances. From the figure inset, the first interception of the data at the high frequency is related to the bulk resistance of about 16 Ω. The diameters of the semicircles in the medium frequency range represent the initial interfacial resistance (33 Ω) and the steady-state interfacial resistance (53 Ω). The t^{+} of the PEO-MIL-53(Al)-LiTFSI electrolyte is 0.343. Without the filler, the t^{+} of the PEO-LiTFSI electrolyte is 0.252. This indicates that the mobility of Li^{+} ions is enhanced due to the function of the metal-organic framework.

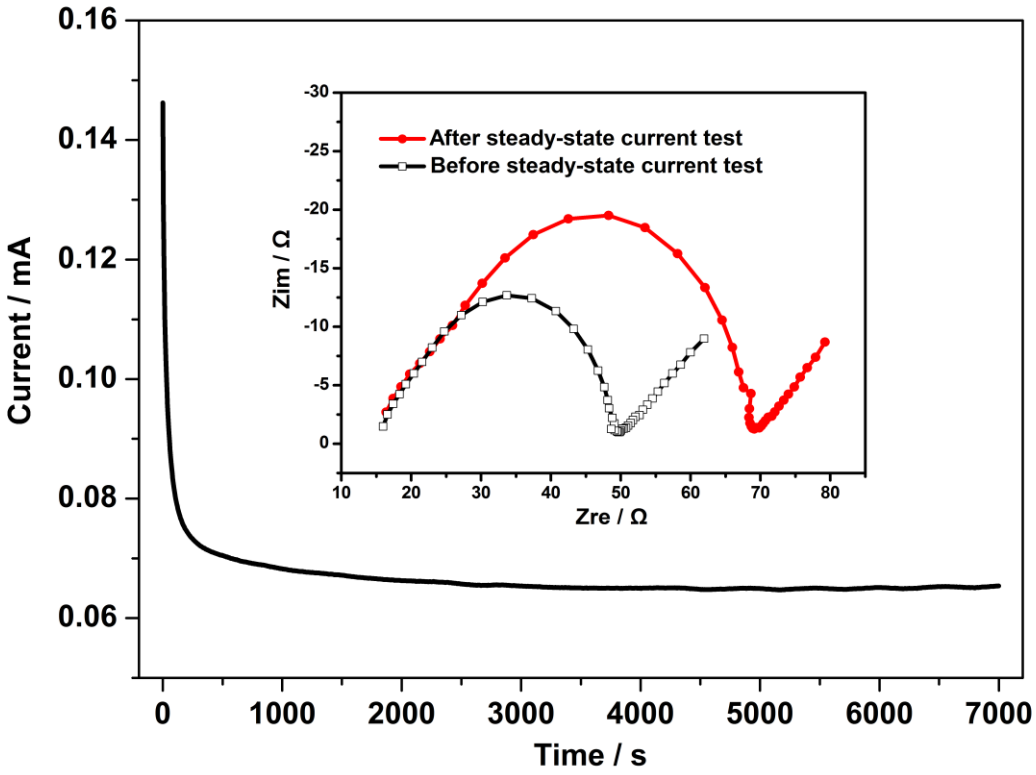

Fig. 3 Chronoamperometry of the Li/PEO-MIL-53(Al)-LiTFSI/Li cells at a potential of 10 mV at 80 ^{o}C. Inset: the AC impedance spectra of the same battery before and after the polarization.

3.3 Lithium ion conduction mechanism for the PEO-MIL-53(Al)-LiTFSI electrolyte

The mechanism for the enhancement of lithium ion transfer properties is preliminarily explored. The Zeta electric potential of the MIL-53(Al) nano particles was measured by Brookhaven Zeta Plus instrument (USA) and the result is shown in Fig. 4. The point of zero charge (PZC) for the particles is at pH 9.1. When pH is lower than 9.1, the Lewis acid property on the surfaces is present. Previous studies found that the ionic conductivity and the lithium ion transference number were increased when adding Lewis acid ceramic nano particles.[33-36] In this study, the pH of the PEO-MIL-53(Al)-LiTFSI electrolyte is about 7, thus, the particles have strong Lewis acid property. Under the condition, the $N(SO_2CF_3)_2^-$ anions of LiTFSI salt may reside on the Lewis acidic surfaces of MIL-53(Al) nano particles, and the Li^+ ions release from the salt and approach the ether oxygen

atoms in PEO chains. This interaction not only disturbs the crystallization of PEO, but also increases the lithium salt dissolution. This experiment demonstrates again that the Lewis acidic nano particles can improve the lithium ionic conductivity in solid polymer electrolyte.

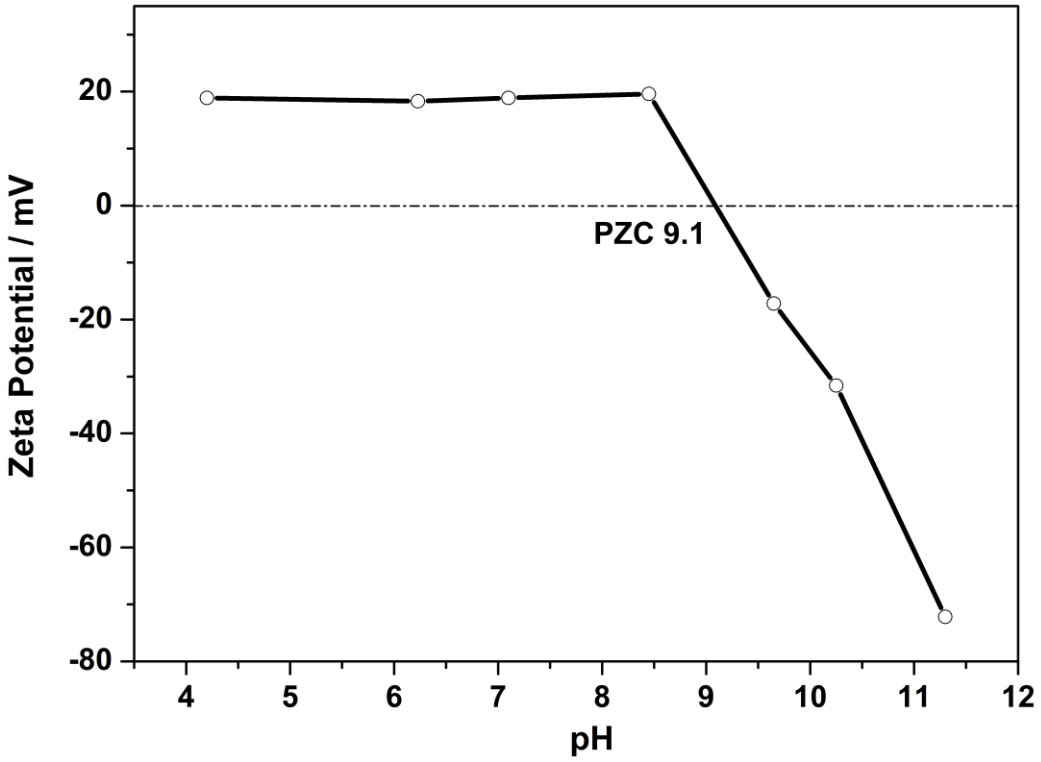

Fig. 4 The zeta electric potential measurement of MIL-53(Al) nano particles.

3.4 Electrochemical stability of the electrolytes

The electrochemical stability of the PEO-LiTFSI electrolyte and the PEO-MIL-53(Al)-LiTFSI electrolyte at 80 ^{o}C and 120 ^{o}C were measured by using linear sweep voltammograms (LSV) in the potential range of 2.5 V to 6.5 V (vs. Li^{+}/Li) (see Fig. 5). The curves present main oxidation decomposition at the potential of 5.31 V at 80 ^{o}C and 5.10 V at 120 ^{o}C for the PEO-MIL-53(Al)-LiTFSI electrolyte. For a comparison, the electrochemical stability of the PEO-LiTFSI electrolyte without MIL-53(Al) was investigated and the lower oxidation potential of

5.15 V at 80 °C and 4.99 V at 120 °C were measured. It is noticed that there is a small current increase about 0.2 mA at 4.5 V at 120 °C. Here, this small current is ignored in the decision of the decomposition potential.

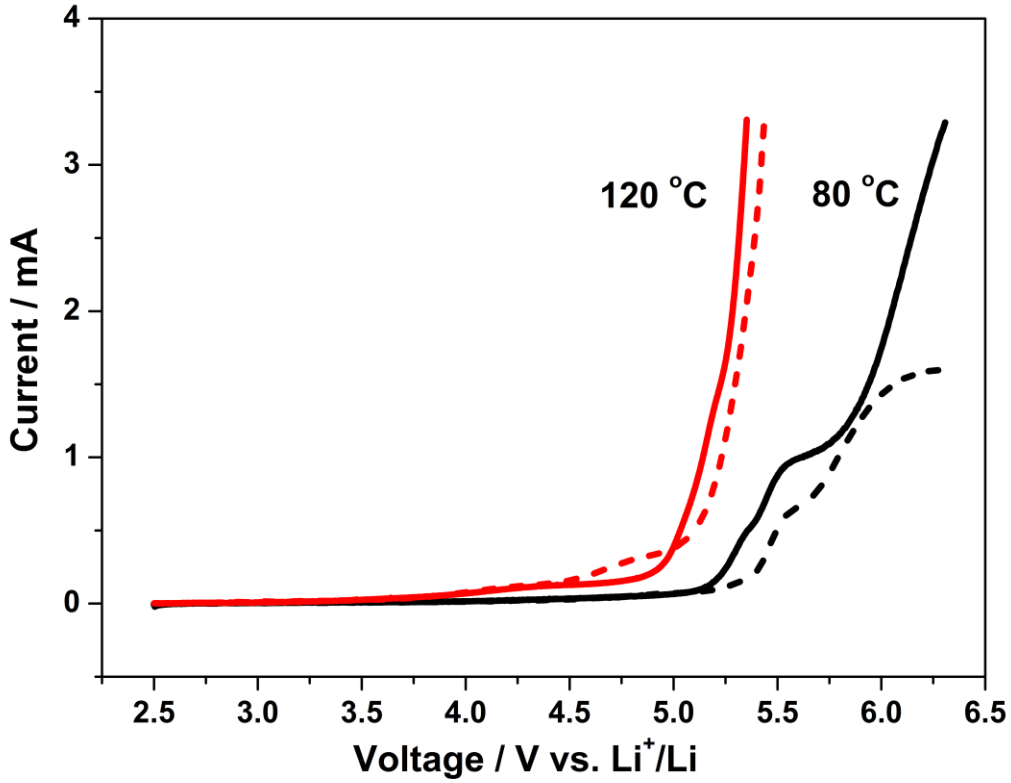

Fig. 5 Linear sweep voltammograms of SS/PEO-LiTFSI/Li (solid line) and SS/PEO-MIL-53(Al)-LiTFSI/Li (dotted line) batteries at 80 °C (black) and 120 °C (red). The electrolytes were sweep in the potential range from 2.5 V to 6.5 V (versus Li/Li^+) at a rate of 10 mVs^{-1}.

3.5 Thermal stability and mechanical characteristic of the electrolytes

The thermal stability of electrolyte is a key factor that determines the safety performance of batteries. Thermo-gravimetric analysis (TG) of the PEO-MIL-53(Al)-LiTFSI electrolyte and the PEO-LiTFSI electrolyte were carried out, and the results are shown in Fig. 6a. By differential processing the TG data, the differential thermo-gravimetric (DTG) curves for the electrolytes are obtained and presented in Fig. 6b. Similar three-step degradations in th temperature range of 48-500 °C for both electrolytes are observed. In the PEO-MIL-53(Al)-LiTFSI electrolyte, the first degradation beginning from 195

°C corresponds to the decomposition of PEO.[37] The second degradation happened at 375 °C is mainly due to the decomposition of LiTFSI.[38] The third one would be also caused by the decomposition of PEO. The residual at 500 °C (about 6%) for the PEO-MIL-53(Al)-LiTFSI electrolyte is from partially carbonized MIL-53(Al).[23] The decomposition peaks in the DTG curve for the PEO-MIL-53(Al)-LiTFSI electrolyte shift right compared to the PEO-LiTFSI electrolyte, especially the LiTFSI decomposition temperature is increased by 15 degrees. Besides, about 1.3% weight loss at 48 °C for both the electrolytes is due to water absorbed during the sample transfer process.

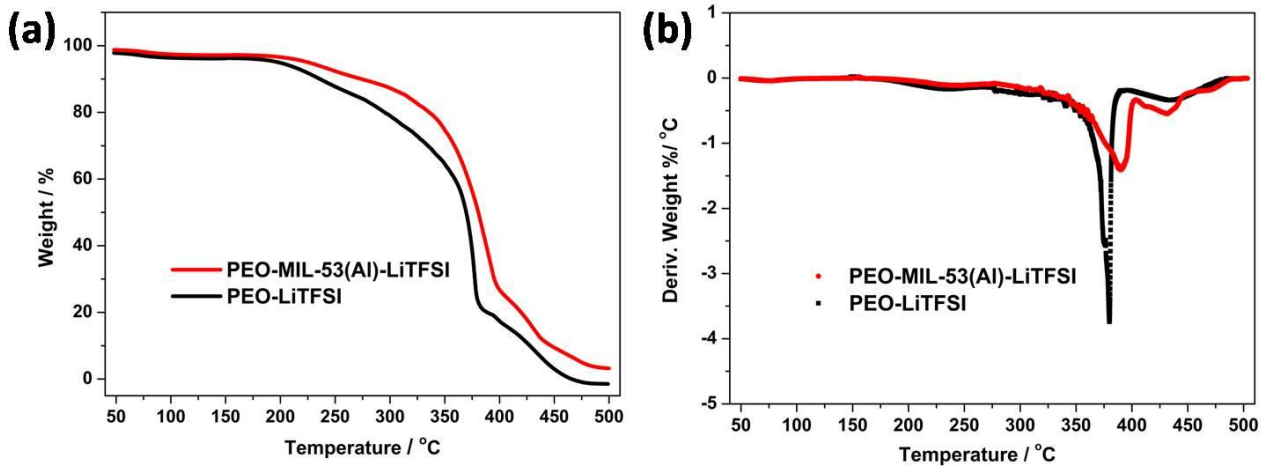

Fig. 6 (a) Thermo-gravimetric analysis of the PEO-LiTFSI and PEO-MIL-53(Al)-LiTFSI electrolytes and (b) DTG curves of the PEO-LiTFSI and PEO-MIL-53(Al)-LiTFSI electrolytes.

In order to characterize the mechanical strength, the dynamic mechanical analysis (DMA) of the PEO-MIL-53(Al)-LiTFSI and PEO-LiTFSI electrolytes was performed. From the stress-strain curves in Fig. 7, the stress of the PEO-MIL-53(Al)-LiTFSI electrolyte is obviously higher than the PEO-LiTFSI electrolyte. The enhancement in the thermal stability and mechanical strength can be attributed to the addition of MIL-53(Al) nano particles which act as crossing-linking centers for PEO, thus a robust network is constructed. These results further demonstrate that the MIL-53(Al) nano particles with Lewis acidic surfaces are benefit for the improvement of solid polymer electrolyte

performance.

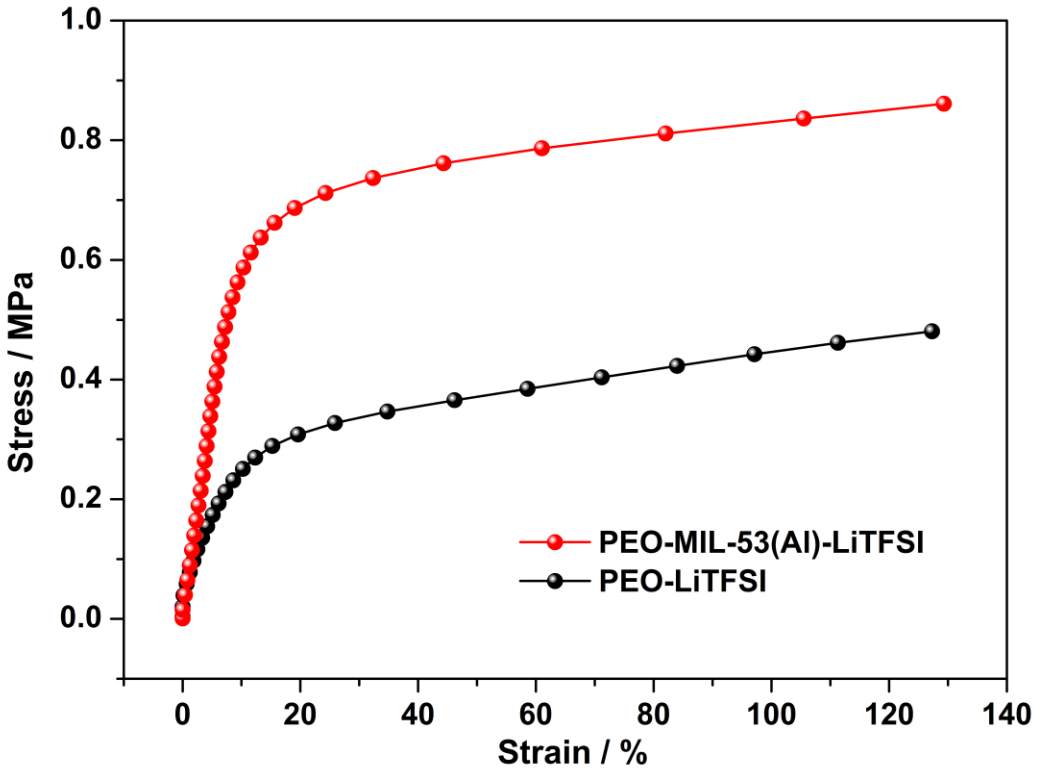

Fig. 7 Stress-strain curves of the PEO-MIL-53(Al)-LiTFSI and PEO-LiTFSI electrolytes.

3.6 Cycling performance of all-solid-state $LiFePO_4$/PEO-MIL-53(Al)-LiTFSI/Li batteries

Fig. 8 shows the cycling performance of the $LiFePO_4$/PEO-MIL-53(Al)-LiTFSI/Li batteries at 5 C, at 80 ^oC and 120 ^oC. For the purpose of retaining high discharge capacities at fast charging/discharging, the batteries were pre charged/discharged at 1 C for about ten cycles (the data are not included in Fig. 8). The initial discharge capacity at 5 C is 127 mAh g^{-1} at 80 ^oC and 136 mAh g^{-1} at 120 ^oC. After 300 cycles, the discharge capacity is 116 mAh g^{-1} at 80 ^oC and 129 mAh g^{-1} at 120 ^oC. In the inset of Fig. 8, when the battery run 610 cycles at 80 ^oC, the retention ratio of the discharge capacity is 80%; when cycled at 120 ^oC, the battery has the discharge capacity of 109 mAh g^{-1} in the 625^{th} cycle with fading of 20%. The batteries were cycled for 1400 cycles at the same rate

and the same temperatures that still have the discharge capacity of 65.9 mAh g^{-1} and 82.9 mAh g^{-1} at 80 ^{o}C and 120 ^{o}C, and the retention ratios are 52.4% and 61.3%, respectively.

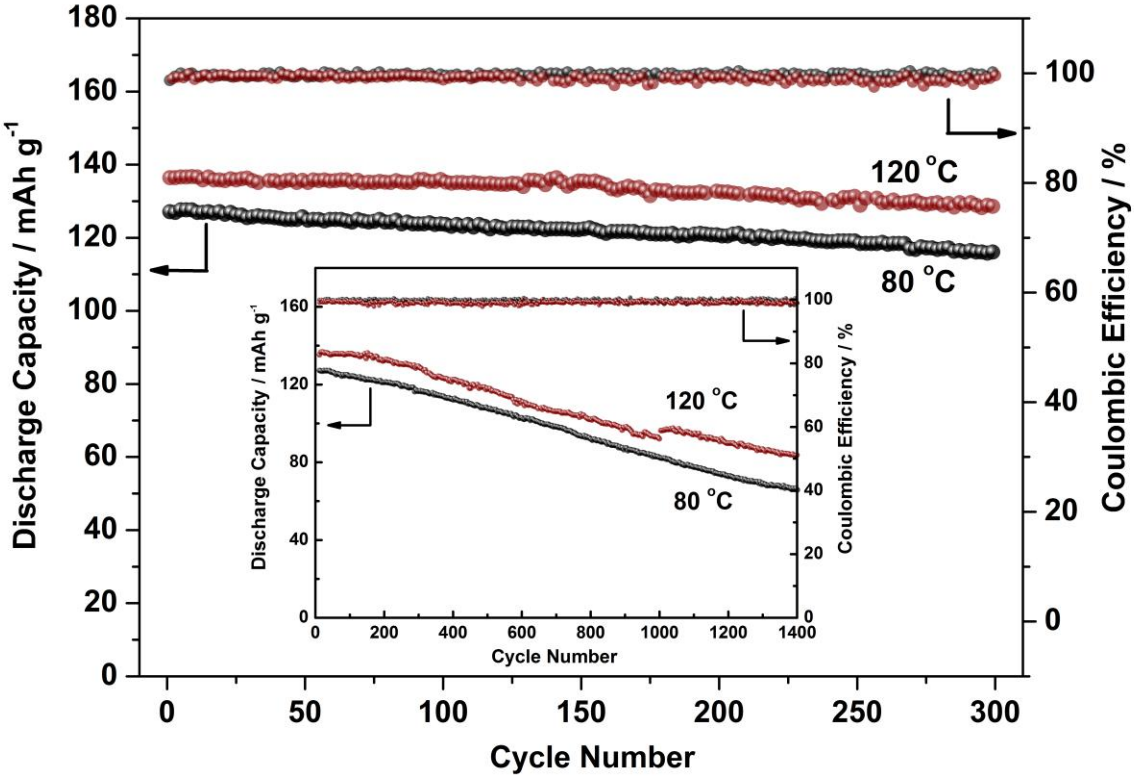

Fig. 8 The cycling performance and Couloumbic efficiencies of the $LiFePO_4$/PEO-MIL-53(Al)-LiTFSI/Li batteries at 5 C, at 80 ^{o}C (black) and 120 ^{o}C (red). Inset: the cycling performance of the same batteries for 1400 cycles. At 120 ^{o}C, an increase in the capacity of about 4.3 mAh g^{-1} in the 1003 cycle is seen since the power system of the computer was broken for 18 h by accident, but the battery was stored in the oven that was kept working at 120 ^{o}C.

In order to further evaluate fast charging/discharging performance, the battery was cycled at 10 C and 120 ℃, and the result is shown in Fig. 9. When cycling at 10 C (about 4 – 5 min for charging or discharging), the battery has the discharge capacity of 116.2 mAh g^{-1} in the first cycle and 103.5 mAh g^{-1} in the 110th cycle that the retention ratio is 90%. At the same temperature and 1 C, another battery can run 530 cycles with the discharge capacity of 129.8 mAh g^{-1}, retaining 90% of the highest discharge capacity (see Fig. 9). Additionally, the inset of Fig. 9 also shows the typical

potential *vs.* time profiles at 1 C, 10 C and 120 °C. Flat voltage plateaus reflecting the insertion/desertion of Li^+ ions in the $LiFePO_4$ cathode are seen. Even in the 110th cycle at 10 C, the plateaus still exist. Compared to all-solid-state lithium ion batteries with PEO based electrolyte reported[10-18], the $LiFePO_4$/PEO-MIL-53(Al)-LiTFSI/Li battery exhibits better cycling performance at high rates and temperatures.

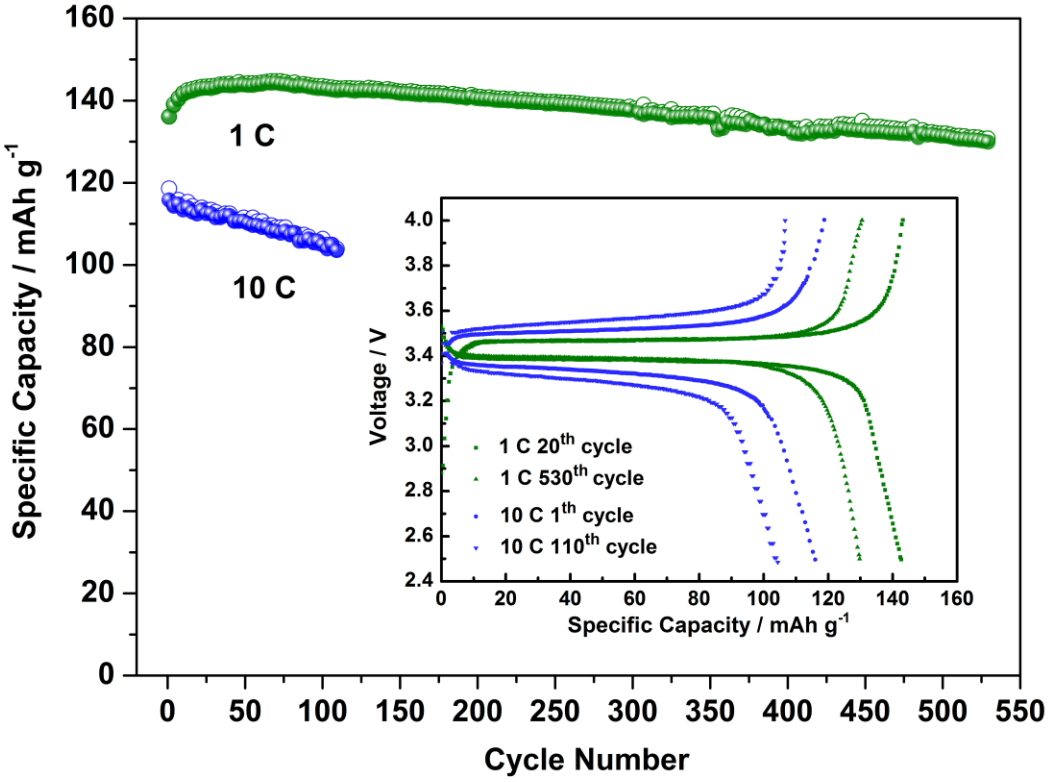

Fig. 9 The charge (hollow circle) and discharge (solid circle) cycling performance of the $LiFePO_4$/PEO-MIL-53(Al)-LiTFSI/Li batteries at 1 C, 10 C at 120 ℃. The cycle number cut off when the testing batteries delivered 90% or less discharge capacity of the highest discharge capacity. Inset: the typical potential *vs.* time profiles at 1 C, 10 C and at 120 °C.

4 Conclusions

A PEO-MIL-53(Al)-LiTFSI electrolyte was prepared by using metal-organic framework MIL-53(Al) as filler for all-solid-state LIBs. The MIL-53(Al) nano particles have Lewis acidic surfaces and interact with $N(SO_2CF_3)_2^-$ anions that promote the dissolution of LiTFSI, thus, the lithium ionic

conductivity is increased. In addition, the particles also act as crossing-linking centers for PEO, which a robust network is built, leading to the increase in thermal stability and mechanical strength. The battery with the electrolyte displays fast charging/discharging abilities. Such electrolyte, which may replace both the separator and liquid electrolyte, can be used directly for fast charging/discharging all-solid-state lithium ion batteries. This is an important step for extending applications of lithium ion batteries.

Acknowledgements

This work was supported by the National Natural Science Foundation of China (No. 51274239) and Central South University, which are greatly appreciated.

References

1 H. J. Zhang, S. Kulkarni and S. L. Wunder, *J. Phys. Chem. B*, 2007, **111**, 3583-3590.
2 J. F. M. Oudenhoven, L. Baggetto and P. H. L. Notten, *Adv. Energy Mater.*, 2013, **1**, 10-13.
3 S. Lee, M. Schomer, H. Peng, K. A. Page, D. Wilms, H. Frey, C. L. Soles and D. Y. Yoon, *Chem. Mater.*, 2011, **23**, 2685-2688.
4 M. Patel, M. U. M. Patel and A. J. Bhattacharyya, *ChemSusChem*, 2010, **3**, 1371-1374.
5 J. Cao, L. Wang, X. M. He, M. Fang, J. Gao, J. J. Li, L. F. Deng, H. Chen, G. Y. Tian, J. L. Wang and S. S. Fan, *J. Mater. Chem. A*, 2013, **1**, 5955-5961.
6 United States Advanced Battery Consortium, *Electric Vehicle Battery Test Procedures Manual*, 1996, Revision 2, Southfield, MI.
7 F. Croce, G. B. Appetecchi, L. Persi and B. Scrosati, *Nature*, 1998, **394**, 456-458.
8 Y. Lin, J. Li, Y. Q. Lai, C. F. Yuan, Y. Cheng and J. Liu, *RSC Adv.*, 2013, **3**, 10722-10730.
9 J. Li, Y. Lin, H. H. Yao, C. F Yuan, and J. Liu, *ChemSusChem*, 2014, 7, 1-9
10 S. T. Ren, H. F. Chang, L. J. He, X. F. Dang, Y. Y Fang, L. Y. Zhang, H. Y. Li, Y. L. Hu and Y. Lin, *J. Appl. Polymer. Sci.*, 2013, **129**, 1131-1142.
11 Y. F. Tong, L. Chen, X. H. He and Y.W. Chen, *Electrochim. Acta*, 2014, **118**, 33-40.
12 Y. H. Li, X. L. Wu, J. H. Kim, S. Xin, J. Su, Y. Yan, J. S. Lee and Y. G. Guo, *J. Power Sources*, 2013, 244, 234-239.
13 J. S. Syzdek, M. B. Armand, P. Falkowski, M. Gizowska, M. Karzowicz, L. Lukaszuk, M. L. Marcinek, A. Zalewska, M. Szafran, C. Masquelier, J. M. Tarascon, W. G. Wieczorek and G. Zukowska, *Chem. Mater.*, 2011, **23**, 1785-1797.
14 J. L. Schaefer, D. A.Yanga and L. A. Archer, *Chem. Mater.*, 2013, **25**, 834-839.
15 R. R. Madathingal and S. L. Wunder, *Macromolecules*, 2011, **44**, 2873-2882.
16 B. W. Zewde, S. Admassie, J. Zimmermann, C. S. Isfort, B. Scrosati and J. Hassoun, *ChemSusChem*, 2013, **6**, 1400-1405.
17 C. F. Yuan, J. Li, P. F. Han, Y. Q. Lai, Z. A. Zhang and J. Liu, *J. Power Sources*, 2013, **240**, 653-658.
18 C. Gerbaldi, J. R. Nair, M. A. Kulandainathan, R. S. Kumar, C. Ferrara, P. Mustarelli and A. M. Stephan, *J. Mater. Chem. A*, 2014, DOI: 10.1039/c4ta01856g.
19 W. J. Rieter, K. M. Pott, K. M. L. Taylor and W. Lin, *J. Am. Chem. Soc.*, 2008, **130**, 11584-11585.
20 K. A. White, D. A. Chengelis, K. A. Gogick, J. Stehman, N. L. Rosi and S. Petoud., *J. Am. Chem. Soc.*, 2009, **131**, 18069-18071.
21 A. J. Lan, K. H. Li, H. H. Wu, D. H. Olson, T. J. Emge, W. Ki, M. C. Hong and J. Li, *Angew. Chem. Int. Ed.*, 2009, **48**, 2334-2338.
22 S. J. Garibay and S. M. Cohen., *Chem. Commun.*, 2010, **46**, 7700-7702.
23 T. Loiseau, C. Serre, C. Huguenard, G. Fink, F. Taulelle, M. Henry, T. Bataille, and G. Fŕey , *Chem. Eur. J.*, 2004, **10**, 1373-1382.
24 J. A. Greathouse and M. D. Allendorf, *J. Am. Chem. Soc.*, 2006, **128**, 10678-10679.
25 B. Kumar, S. J Rodrigues and S. Koka, *Electrochim. Acta*, 2002, **47**, 4125-4131.
26 Y. H. Li, X. L. Wu, J. H. Kim, S. Xin, J. Su, Y. Yan, J. S. Lee and Y. G. Guo, *J. Power Sources*, 2013, **244**, 234-239.
27 R.S. Bobadea, S.V. Pakade and S. P. Yawale, *J. Non-Cryst Solids*, 2009, **355**, 2410-2414.
28 F. B. Dias, L. Plomp and J. J. B. Veldhuis, *J. Power Sources*, 2000, **88**, 169-191.
29 C. D. Robitaille and D. Fauteux, *J. Electrochem. Soc.*, 1986, **133**, 315-325.
30 M. Doyle, T. F. Fuller and J. Newman, *Electrochim. Acta*, 1994, **39**, 2073-2081.
31 K. E. Thomas, S. E. Sloop, J. B. Kerr and J. Newman, *J. Power Sources*, 2000, **89**, 132-138.
32 J. Evans, C. A. Vincent and P. G. Bruce, *Polymer*, 1987, **28**, 2324-2328.

33 F. Croce, L. Persi, B. Scrosati, F. S. Fiory, E. Plichta, and M. A. Hendrickson, *Electrochimi. Acta* 2001, **46**, 2457-2461.
34 W. Wieczorek, Z. Florjancyk and J. R. Stevens, *Electrochim. Acta*, 1995, **40**, 2251.
35 F. Croce, R. Curini, A. Martinelli, L. Persi, F. Ronci and B. Scrosati, *J. Phys. Chem.*, 1999, **103**, 10632-10638.
36 N. Angulakshmi, K. S. Nahm, J. R. Nair, C. Gerbaldi, R. Bongiovanni, N. Penazzi and A. M. Stephan, *Electrochim. Acta*, 2013, 90, 179-185.
37 T. Shodai, B. B. Owens, T. Ostsuka, J. Yamaki, *J. Electrochem. Soc.*, 1994, **141**, 2978-2981.
38 M. Echeverri, N. Kim and T. Kyu, *Macromolecules*, 2012, **45**, 6068-6077.

A fast charging/discharging all-solid-state lithium ion battery based on PEO-MIL-53(Al)-LiTFSI thin film electrolyte

Kai Zhu, Yexiang Liu and Jin Liu*

School of Metallurgy and Environment, Central South University, Changsha City, 410083, China

*Corresponding author: Jin Liu
Email: jinliu@csu.edu.cn

Abstract

Metal-organic framework aluminum 1,4-benzenedicar-boxylate (MIL-53(Al)) is used as a filler for polyethylene oxide (PEO) based thin film electrolyte. With the participation of MIL-53(Al), the ionic conductivity of this electrolyte is increased from 9.66×10^{-4} S cm^{-1} to 3.39×10^{-3} S cm^{-1} at 120 ^{o}C and the electrochemical window is raised from 4.99 V to 5.10 V. Besides, the all-solid-state $LiFePO_4$/Li battery based on the electrolyte was fabricated. At 5 C and 120 ^{o}C, the battery delivers the discharge capacity of 136 mAh g^{-1} in the initial cycle, 129 mAh g^{-1} in the 300th cycle, and 83.5 mAh g^{-1} in the 1400th cycle. At 10 C and 120 ^{o}C, its discharge capacity is 116.2 mAh g^{-1} in the initial cycle and 103.5 mAh g^{-1} in the 110th cycle. The results indicate that the metal-organic framework is a novel structural modifier for solid polymer electrolyte in fast charging/discharging lithium ion batteries.

TOC